DOI: 10.1021/ic100887c

Inorganic Chemistry
Article

Hydrothermal Synthesis of Uranyl Squarates and Squarate-Oxalates: Hydrolysis Trends and in Situ Oxalate Formation

Clare E. Rowland and Christopher L. Cahill*

Contribution from the Department of Chemistry, The George Washington University, 725 21st St. NW, Washington, DC 20052

Received May 5, 2010

We report the synthesis of two uranyl squarates and two mixed-ligand uranyl squarate−oxalates from aqueous solutions under hydrothermal conditions. These products exhibit a range of uranyl building units from squarates with monomers in $(UO_2)_2(C_4O_4)_5 \cdot 6NH_4 \cdot 4H_2O$ (**1**; $a = 16.731(17)$ Å, $b = 7.280(8)$ Å, $c = 15.872(16)$ Å, $\beta = 113.294(16)°$, monoclinic, $P2_1/c$) and chains in $(UO_2)_2(OH)_2(H_2O)_2(C_4O_4)$ (**2**; $a = 12.909(5)$ Å, $b = 8.400(3)$ Å, $c = 10.322(4)$ Å, $\beta = 100.056(7)°$, monoclinic, $C2/c$) to two squarate−oxalate polymorphs with dimers in $(UO_2)_2(OH)(C_4O_4)(C_2O_4) \cdot NH_4 \cdot H_2O$ (**3**; $a = 9.0601(7)$ Å, $b = 15.7299(12)$ Å, $c = 10.5108(8)$ Å, $\beta = 106.394(1)°$, monoclinic, $P2_1/n$; and **4**; $a = 8.4469(6)$ Å, $b = 7.7589(5)$ Å, $c = 10.5257(7)$ Å, $\beta = 105.696(1)°$, monoclinic, $P2_1/m$). The dominance at low pH of monomeric species and the increasing occurrence of oligomeric species with increasing pH suggests that uranyl hydrolysis, $m{UO_2}^{2+} + nH_2O \rightleftharpoons [(UO_2)_m(OH)_n]^{2m-n} + nH^+$, has a significant role in the identity of the inorganic building unit. Additional factors that influence product assembly include in situ hydrolysis of squaric acid to oxalic acid, dynamic metal to ligand concentration, and additional binding modes resulting from the introduction of oxalate anions. These points and the effects of uranyl hydrolysis with changing pH are discussed in the context of the compounds presented herein.

Introduction

Two primary factors influence product formation in uranyl-organic hybrid materials: the speciation of the uranyl cation and the organic linker's "bite" and "bend." Hydrolysis affects the identity of the inorganic building unit, for which monomeric species to oligomeric clusters of up to six uranyl cations have been observed.[1,2] Further polymerization may result in species with chains, ribbons, or sheets of uranyl cations, as seen in minerals and related compounds.[3,4] The driving force in solution behind this oligomerization is hydrolysis, the equation for which is shown here:

$$m{UO_2}^{2+} + nH_2O \rightleftharpoons [(UO_2)_m(OH)_n]^{2m-n} + nH^+ \qquad (1)$$

We have previously explored the effects of hydrolysis under ambient conditions on the building unit observed in the solid state as a function of pH,[5] an increase in which we would expect to favor hydrolysis and thus oligomerization. Hydrolysis under hydrothermal conditions, as discussed herein, has been studied much less, and while extensive speciation diagrams for the uranyl cation exist for ambient conditions, the species present under hydrothermal conditions are not entirely agreed upon.[6] Nonetheless, it has been reasonably well established that monomeric hydrolysis species are favored by increasing temperature.[6−8] This is not to say, however, that monomeric species exist to the exclusion of oligomers at higher pH.[7,8]

The second factor that determines the reaction product is the "bite" and "bend" of the ligand, in other words, the coordination mode that the ligand adopts and ligand's rigidity or flexibility, both of which contribute to the final structure.[9] A ligand like squaric acid (Scheme 1a) exhibits a variety of binding modes—from monodentate to tetrakismonodentate on a wide variety of metals to bidentate on a smaller subset including the lanthanides—on a rigid molecule.[10] It also has

*To whom correspondence should be addressed. Phone: (202)994-6959. E-mail: cahill@gwu.edu.

(1) Cahill, C.; de Lill, D.; Frisch, M. *Cryst. Eng. Comm.* **2007**, *9*, 15–26.
(2) Thuéry, P.; Nierlich, M.; Souley, B.; Asfari, Z.; Vicens, J. *Dalton Trans.* **1999**, 2589–2594.
(3) Duvieubourg, L.; Nowogrocki, G.; Abraham, F.; Grandjean, S. *J. Solid State Chem.* **2005**, *178*, 3437–3444.
(4) Burns, P. C. *Can. Mineral* **2005**, *43*, 1839–1894.
(5) Rowland, C. E.; Cahill, C. L. *Inorg. Chem.* **2010**, in press.
(6) Grenthe, I.; Fuger, J.; Konings, R. J. M.; Lemire, R. J.; Muller, A. B.; Nguyen-Trung, C.; Wanner, H. *Chemical Thermodynamics of Uranium*, 2nd ed.; Nuclear Energy Agency, Organisation for Economic Co-operation and Development: Paris, 2004.
(7) Zanonato, P.; Di Bernardo, P.; Bismondo, A.; Liu, G.; Chen, X.; Rao, L. *J. Am. Chem. Soc.* **2004**, *126*, 5515–5522.
(8) Kirishima, A.; Kimura, T.; Tochiyama, O.; Yoshida, Z. *J. Alloys Compd.* **2004**, *374*, 277–282.
(9) Cahill, C. L.; Borkowski, L. A. U(VI)-containing metal-organic frameworks and coordination polymers. In *Structural Chemistry of Inorganic Actinide Compounds*; Krivovichev, S. V., Burns, P. C., Tananaev, I., Eds.; Elsevier: Amsterdam, 2006.
(10) Hall, L. A.; Williams, D. J. *Adv. Inorg. Chem.* **2001**, *52*, 249–291.

Published on Web 06/16/2010

Scheme 1. (a) Squaric Acid and (b) Oxalic Acid

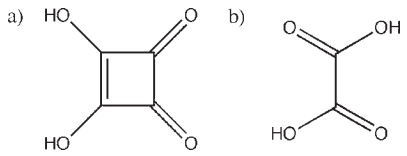

demonstrated success in forming hybrid materials with f elements[5,11,12] and is therefore our ligand of choice in this study of the solid state expression of uranyl hydrolysis.

A third variable influencing product formation that arises with less frequency is an in situ reaction to form a ligand that was not among the original starting materials.[13,14] Newly generated reagents may result in the formation of products that were otherwise inaccessible[15,16] or may introduce a second ligand to the system which coordinates to the metal center concurrently with the first.[17] The presence of ligands formed during the in situ reaction may further introduce modes of coordination that were not previously available, contributing to diversity in product formation. For example, in situ hydrolysis of squaric acid to oxalic acid (Scheme 1b) has been observed previously[18−22] and opens the possibility of bidentate coordination (i.e., chelation) to the uranyl cation, a binding mode not known to occur with uranyl squarates.

Herein, we investigate the solid state expression of hydrolysis through hydrothermal synthesis of uranyl−organic hybrid materials. In more general terms, the study of such compounds and, in particular, behavior of the uranyl cation and its interactions with organic compounds under environmentally relevant conditions is fundamental to improving our understanding of all aspects of the nuclear fuel cycle. We report the uranyl building units that we observe in crystalline reaction products of the uranyl cation and squaric acid as a function of pH and temperature. We not only observe a variety of inorganic hydrolysis products but also report the formation of squarate−oxalates through partial in situ hydrolysis of the behavior ligand. Two novel uranyl squarates have been synthesized, $(UO_2)_2(C_4O_4)_5\cdot 6NH_4\cdot 4H_2O$ (**1**) and $(UO_2)_2(OH)_2(H_2O)_2(C_4O_4)$ (**2**), in addition to two uranyl squarate−oxalate polymorphs, $(UO_2)_2(OH)(C_4O_4)(C_2O_4)\cdot NH_4\cdot H_2O$ (**3** and **4**). In a systematic study of product formation as a function of pH and temperature, we have additionally observed several previously reported uranyl squarates[5,12] and uranyl oxalates.[3,23] As such, we shall discuss the effects of uranyl hydrolysis on solid state reaction products in the context of **1**−**4** and these other squarates and oxalates.

Experimental Section

Synthesis. ***Caution!*** *While the uranyl nitrate, $UO_2(NO_3)_2$, used in these experiments contained depleted uranium, standard precautions for handling radioactive material should be observed.* All materials used in the synthesis are available commercially and were used as received.

Hydrothermal reactions of uranyl nitrate hexahydrate and squaric acid were prepared in 1:1 and 1:2 molar ratios and explored as a function of pH through the addition of 9.6 N ammonium hydroxide in incremental amounts (0, 100, 200, 300, 400, 500 μL of 9.6 N NH_4OH for 1:1; 0, 200, 400, 600, 700, 800 μL for 1:2). These additions of NH_4OH resulted in a pH range of $1 < pH < 9$ at the beginning of synthesis. Each pH series was repeated at 90, 120, and 150 °C, corresponding to autogenous pressures of approximately 1−5 atm. Unless otherwise specified, approximately 1.5 mL of H_2O acted as a solvent. At 120 °C in a 1:2 molar ratio, however, lower solvent volumes (i.e., 0.25 mL) were found to be optimal for crystal growth.

Hydrothermal reactions were prepared by sealing the reactants in a 23 mL Teflon-lined Parr bomb and placing them in an isothermal oven for 3 days, after which time the bomb was removed and left on the bench to cool to room temperature over approximately 8 h. The mother liquor was decanted, and the remaining solids were washed in water and ethanol. Although none of the products were obtained as pure phases, optimal conditions for synthesis of the novel compounds reported in this study are summarized in Table 1. Optimization reflects both the growth of crystals suitable for single-crystal X-ray diffraction and contribution by the compound to the powder X-ray diffraction pattern.

X-Ray Structure Determination. Single crystals from each preparation were isolated from the bulk reaction product and mounted on a MicroMount needle (MiTeGen). Reflections were collected from 0.5° φ and ω scans at 100 K on a Bruker SMART diffractometer with an APEXII CCD detector and a Mo Kα source. The APEXII software suite[24] was used to integrate the data and apply an absorption correction.[25] Structures were solved using direct methods and refined with SHELX-97.[26] Publication materials were prepared using the WinGX software suite,[27] and figures were made with CrystalMaker.[28]

H atoms were located in difference Fourier maps but could not be satisfactorily refined for any of the compounds. Ambiguity in the position of H atoms on solvent water molecules and ammonium cations prevented assignment, and H on hydroxyl groups and bound water molecules coordinated to U were not evident in the difference Fourier maps and were therefore not assigned. Bond valence summation (Supporting Information, SI 1) was used to distinguish between water and hydroxyl oxygen atoms. Crystallographic data for **1**−**4** are summarized in Table 2.

Positional disorder in the one of the three squarate anions in **1** required the use of a PART command to resolve the disordered segments. Refinement revealed that each part was approximately 50% occupied.

Initial indexing of **3** yielded a unit cell with half the volume that we report here. The result of this smaller cell was the superimposition of electron density from two uranyl cations with differing orientation. Doubling the *b* axis allowed the superimposed data to be resolved and permitted solution and refinement of the structure reported here. Disagreeable thermal parameters persisted for the ammonium cation (N1) in the structure and required that it be refined isotropically, as anisotropic refinement resulted in nonpositive definite thermal parameters.

(11) Petit, J.-F.; Gleizes, A.; Trombe, J.-C. *Inorg. Chim. Acta* **1990**, *167*, 51–68.
(12) Wilson, A. S. *Cryst. Struct. Comm.* **1982**, *11*, 809–13.
(13) Zhang, X.-M. *Coord. Chem. Rev.* **2005**, *249*, 1201–1219.
(14) Chen, X.-M.; Tong, M.-L. *Acc. Chem. Res.* **2006**, *40*, 162–170.
(15) Rowland, C. E.; Belai, N.; Knope, K. E.; Cahill, C. L. *Cryst. Growth Des.* **2010**, *10*, 1390–1398.
(16) Knope, K. E.; Cahill, C. L. *Inorg. Chem.* **2008**, *47*, 7660–7672.
(17) Knope, K. E.; Cahill, C. L. *Inorg. Chem.* **2007**, *46*, 6607–6612.
(18) Heinl, U.; Hinse, P.; Mattes, R. *Z. Anorg. Allg. Chem.* **2001**, *627*, 2173–2177.
(19) Yeşilel, O. Z.; Erer, H.; Odabaşoğlu, M.; Büyükgüngör, O. *J. Inorg. Organomet. Polym.* **2010**, *20*, 78–82.
(20) Piggot, P. M. T.; Hall, L. A.; White, A. J. P.; Williams, D. J. *Inorg. Chim. Acta* **2004**, *357*, 250–258.
(21) Dan, M.; Rao, C. N. R. *Solid State Sci.* **2003**, *5*, 615–620.
(22) Trombe, J.-C.; Petit, J.-F.; Gleizes, A. *Eur. J. Solid State Inorg. Chem.* **1991**, *28*, 669–681.
(23) Jayadevan, N. C.; Chackraburtty, D. M. *Acta Crystallogr., Sect. B* **1972**, *28*, 3178–3182.
(24) *APEXII Software Suite*, 2008.3−0; Bruker AXS: Madison, WI, 2008.
(25) Sheldrick, G. *SADABS*, 2008/1; University of Gottingen: Gottingen, Germany, 2008.
(26) Sheldrick, G. *Acta Crystallogr., Sect. A* **2008**, *64*, 112–122.
(27) Farrugia, L. *J. Appl. Crystallogr.* **1999**, *32*, 837–838.
(28) Palmer, D. *CrystalMaker for Mac OS X*, 8.2.2; CrystalMaker Software Limited: Bicester, England, 2009.

Table 1. Synthetic Conditions for **1**−**4**

	1	**2**	**3**	**4**
$UO_2(NO_3)_2 \cdot 6H_2O$ (g; mmol)	0.250; 0.50	0.249; 0.50	0.250; 0.50	0.250; 0.50
$C_4H_2O_4$ (g; mmol)	0.114; 1.0	0.058; 0.50	0.058; 0.50	0.055; 0.48
H_2O (g; mmol)	0.26; 15	1.56; 87	1.50; 87	1.50; 87
NH_4OH (μL; mmol)	350; 3.8	400; 4.3	350; 3.8	350; 3.8
pH_i	5.85	6.05	3[a]	4[a]
pH_f	5.47	5.28	2[a]	1[a]
temperature (°C)	120	90	150	150
time (days)	3	3	10	1
other phases[b]	Sq1, Sq2	**4**	Sq1	Sq1, Ox2

[a] Measurement with pH paper rather than electrode. [b] Refer to Table 4 for explanation of abbreviations.

Table 2. Summary of Crystallographic and Structure Refinement Data from **1**−**4**

	1	**2**	**3**	**4**
empirical formula	$C_{10}H_{16}N_3O_{14}U$	$C_2H_3O_6U$	$C_6H_7NO_{14}U_2$	$C_6H_7NO_{14}U_2$
fw	640.29	359.055	793.176	793.176
temp (K)	100	100	100	100
λ (Mo Kα)	0.71073	0.71073	0.71073	0.71073
cryst syst	monoclinic	monoclinic	monoclinic	monoclinic
space group	$P2_1/c$	$C2/c$	$P2_1/n$	$P2_1/m$
color	red	yellow	yellow	yellow
habit	block	block	block	block
a (Å)	16.731(17)	12.909(5)	9.0601(7)	8.4469(6)
b (Å)	7.280(8)	8.400(3)	15.7299(12)	7.7589(5)
c (Å)	15.872(16)	10.322(4)	10.5108(8)	10.5257(7)
α (deg)	90	90	90	90
β (deg)	113.294(16)	100.056(7)	106.394(1)	105.696(1)
γ (deg)	90	90	90	90
V (Å^3)	1776(3)	1102.1(7)	1437.04(19)	664.12(8)
Z	4	8	4	2
D_{calc} (g·cm^{-3})	2.395	4.340	3.642	3.927
μ (mm^{-1})	9.222	29.413	22.587	24.433
R_{int}	4.36%	7.60%	3.05%	3.22%, 3.63%[a]
R_1[b] [$I > 2\sigma(I)$]	2.38%	3.11%	1.80%	3.82%
wR_2[b] [$I > 2\sigma(I)$]	5.43%	5.81%	4.03%	9.64%

[a] Pseudomerohedral twin integrated on two domains; R_{int} is reported for each domain separately. [b] $R_1 = \sum||F_o| - |F_c||/\sum|F_o|$; $wR_2 = (\sum[w(F_o^2 - F_c^2)^2/\sum[w(F_o^2)^2])^{1/2}$.

Initial determination of the Bravais lattice of **4** yielded an orthorhombic cell. Refinement of the structure in space group *Pmmm* resulted in improbable coordination geometry about the uranyl cation. Careful reassessment of the reflections in a reciprocal lattice viewer revealed two superimposed lattices, which were also observed in three other crystals of **4**. Manual selection of reflections from one of these lattices allowed indexing that resulted in a monoclinic cell. Both the consistent appearance of two domains among multiple crystals and the indexing to a higher symmetry lattice type suggested pseudomerohedral twinning. CELL_NOW was used to find and index the separate domains,[29] and integration, solution, and refinement followed as for a nonmerohedral twin. Disagreeable thermal parameters for the solvent water molecule (OW1) required that it be refined isotropically, as anisotropic refinement resulted in nonpositive definite thermal parameters.

Powder X-ray diffraction data were collected on a Rigaku Miniflex diffractometer (Cu Kα, 3−60°) and analyzed with the Jade software package.[30] Calculated powder patterns were overlaid on observed patterns to identify phases present.

Results

Structure Descriptions. The crystal structure of **1** is composed of monomeric uranyl building units linked by bismonodentate squarate anions to form sheets (Figure 1). The uranyl cation (O8−U1−O9) is coordinated to three crystallographically unique squarate anions through atoms O1, O2, and O4. The remaining two oxygen atoms in the inner coordination sphere of the uranyl cation (O3 and O12^i; i = x, $y - 1$, z) are also contributed by the squarate anions (Figure 2). The first squarate anion (C11−C14; O1, O12−O14) is coordinated to uranyl cations through O1 and O12. The second squarate anion (C21−C24; O2, O22, O3, O24) bridges uranyl centers through O2 and O3, which are located on opposite "corners" of the squarate anion. This ligand displays some structural disorder, which is modeled through a secondary ring with designation "a" (e.g., C24a). The final squarate anion sits on an inversion center and consists of O4, C41, C42, O42, and the symmetry equivalents of each, generated by operator $-x + 1$, $y - 1/2$, $-z + 1/2$. The extended structure is a two-dimensional sheet, shown in Figure 1a. Two solvent water molecules and three charge-balancing ammonium cations occupy the interlayer (Figure 1b). Placement of hydrogen atoms on both water molecules and ammonium cations proved ambiguous, and they were therefore not modeled. Selected bond distances and angles appear in Table 3.

The crystal structure of **2** consists of chains of point-sharing pentagonal bipyramids linked by squarate anions into sheets (Figure 3a). Each uranyl cation (O5−U1−O6) has five oxygen atoms bound in the equatorial plane, of which four are crystallographically unique (O1, O2, O3, O4) and one (O3^{iii}) is generated through the symmetry

(29) Sheldrick, G. *Cell_Now*; Bruker-AXS: Madison, WI, 2004.
(30) *JADE*, 6.1; Materials Data, Inc: Livermore, CA, 2002.

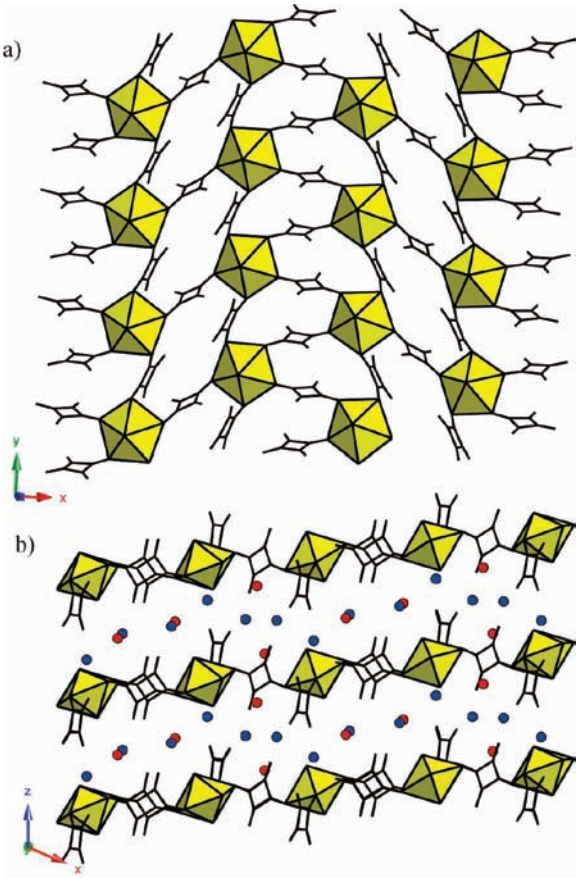

Figure 1. (a) The sheet of **1**, composed of uranyl centers linked by squarate anions and seen here in the [001] direction. (b) The interlayer, here viewed in the [010] direction, containing molecules of solvent water (red) and ammonium (blue).

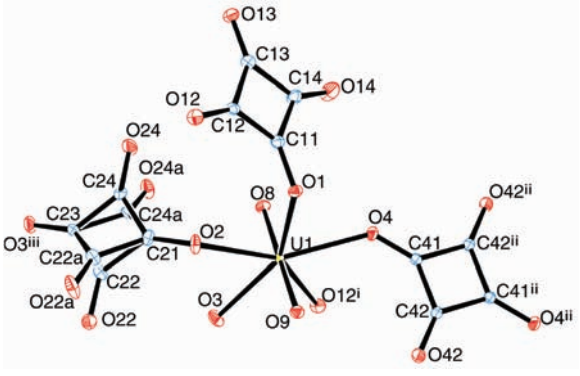

Figure 2. A thermal ellipsoid plot (50% probability) showing the local coordination of the squarate anions to the uranyl center. Hydrogen atoms and solvent water molecules have been omitted for clarity. Symmetry transformations: i = $x, y - 1, z$; ii = $-x + 1, y - 1/2, -z + 1/2$; iii = $x, y + 1, z$.

transformation $-x + 1, -y, -z + 2$ (Figure 3b). Pentagonal bipyramids are point-sharing through hydroxyl oxygen O3. Bond valence summation suggests that O4 is a bound water molecule (Supporting Information, SI 1), which is consistent with a charge-balanced formula. The squarate anion is coordinated to the uranyl cation through O1 and O2; C1 and C2 together with symmetry-generated $C1^{ii}$ and $C2^{ii}$ ($-x + 1/2, y - 1/2, -z + 3/2$) form the four-membered squarate ring. The squarate anions are tetrakismonodentate, bridging adjacent uranyl cations through O1 and O2 and

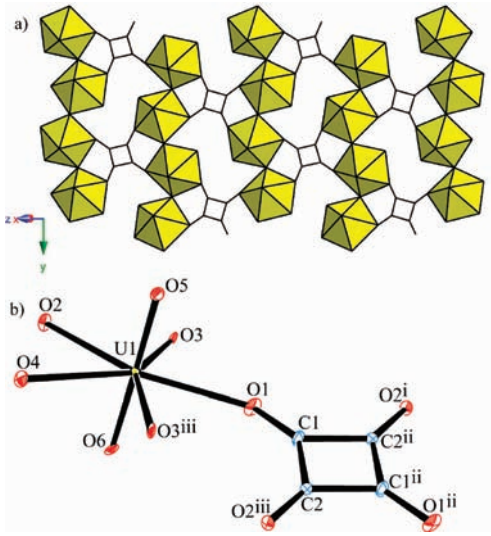

Figure 3. (a) View along [10−1] showing two-dimensional sheets of point-sharing uranyl chains linked by squarate anions. (b) Local coordination environment of **2** represented here as a thermal ellipsoid plot with probability level at 50%. Hydrogen atoms have been omitted for clarity. Symmetry transformations i = $-x + 1/2, y + 1/2, -z + 3/2$; ii = $-x + 1/2, y - 1/2, -z + 3/2$; iii = $-x + 1, -y, -z + 2$.

Table 3. Important Bond Distances (Å) and Angles (deg) in **1**−**4**

	1	**2**	**3**	**4**
U═O	1.773(3)	1.772(6)	1.770(3)	1.789(9)
O═U═O	178.70(13)	178.3(3)	178.91(15)	179.8(4)
U−O	2.389(3)	2.395(6)	2.404(3)	2.390(8)
C−C (squarate)	1.469(11)	1.452(12)	1.466(7)	1.454(17)
C−C (oxalate)			1.538(6)	1.543(16)
C−O (squarate)	1.260(11)	1.256(10)	1.255(6)	1.252(10)
C−O (oxalate)			1.253(6)	1.260(9)
O−C−C (squarate)	135.0(9)	135.1(8)	135.0(5)	135.0(7)
Mean; min; max	131.1(4)	130.1(8)	132.9(5)	131.8(7)
	138.6(7)	139.4(2)	137.1(4)	137.9(7)
O−C−C (oxalate)			116.0(4)	116.2(5)
Mean; min; max			115.1(4)	116.0(4)
			116.4(4)	116.4(5)

bridging chains to form the extended sheet (Figure 3a). Selected bond distances and angles appear in Table 3.

The crystal structure of **3** is defined by point-sharing dimers bound by squarate and oxalate anions into sheets (Figure 4a). Two crystallographically unique U(VI) metal centers exist as point-sharing dimers, each with the characteristic uranyl oxygen atoms (O6−U1−O7; O16−U2−O17). As shown in Figure 4b, O1 and O2 on U1 are bound to C1 and C2 of the bisbidentate oxalate anion. The oxalate is further coordinated to U2 via O11 and O12. O4 bridges U1 and U2. The remaining oxygen atoms in the coordination spheres of U1 (O3, O5) and U2 (O13, O14) are contributed by the tetrakismonodentate squarate anion, the carbon ring of which is composed of C3−C6. The uranyl dimers are bridged by the squarate and oxalate anions to form sheets, as shown in Figure 4a. One solvent water molecule (OW1) and one ammonium cation (N1) occupy the interlayer region and are aligned with intralayer void spaces. Selected bond distances and angles appear in Table 3.

The crystal structure of **4** is very similar to that of **3**; it is likewise composed of point-sharing uranyl dimers which are bridged through squarate and oxalate anions to form

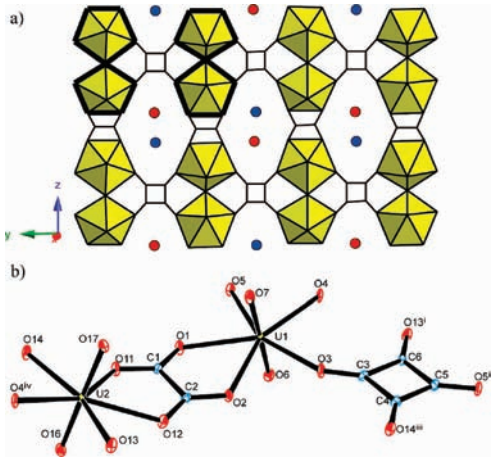

Figure 4. (a) A view down [100] shows the topology of **3**. Uranyl dimers are coordinated by bridging squarate and oxalate anions. Solvent water (red) and ammonium cations (blue) occupy void space between sheets. A uranyl dimer has been outlined in bold to facilitate discussion of cation orientation. (b) The local coordination geometry of **3**, represented here as a 50% probability thermal ellipsoid plot, shows two unique metal centers coordinated to squarate and oxalate anions. Hydrogen atoms and solvent water molecules and ammonium cations have been omitted for clarity. Symmetry transformations: i = $x, y, z + 1$; iii = $-x + 3/2, y + 1/2, -z + 7/2$; iv = $x, y, z - 1$.

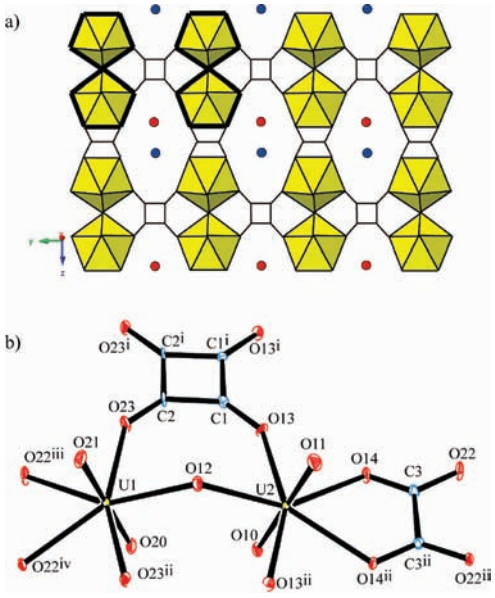

Figure 5. (a) A view down [100] showing the topology of **4**. Uranyl dimers are coordinated by bridging squarate and oxalate anions. Solvent water (red) and ammonium cations (blue) occupy void space between sheets. A uranyl dimer has been outlined in bold to facilitate discussion of cation orientation. (b) The local coordination geometry of **4**, represented here as a 50% probability thermal ellipsoid plot, shows two unique metal centers coordinated to squarate and oxalate anions. Solvent water molecules and ammonium cations have been omitted for clarity. Symmetry transformations: i = $-x, -y, -z$; ii = $-x, y + 1/2, -z$; iii = $x, y, z - 1$; iv = $x, -y + 1/2, z$.

sheets (Figure 5a). Two crystallographically unique uranyl cations (O10−U1−O11; O20−U2−O21) each have two equatorial oxygen atoms contributed by a squarate anion (O13 and O13^{ii} for U1, O23 and O23^{ii} for U2; ii = $-x, y + 1/2$) and two contributed by an oxalate anion (O14 and O14^{ii} for U1, O22^{iii} and O22^{iv} for U2; iii = $x, y, z - 1$; iv = $x, -y + 1/2, z$). The remaining oxygen atom, O12, is a

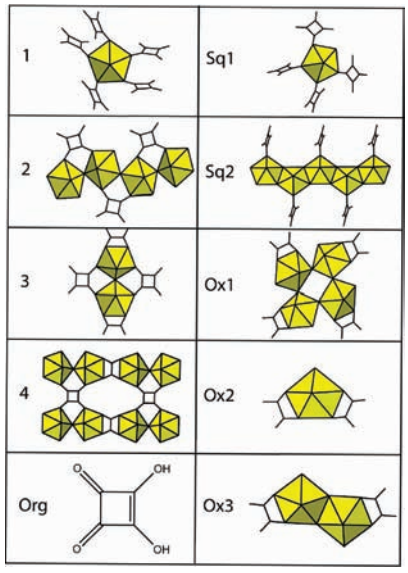

Figure 6. Key for local structures shown in Figures 7−9. References for these structures may be found in Table 4.

Table 4. Previously Reported Crystal Structures Cited in This Work[a]

abbreviation	reference	CSD/ICSD	building unit
Sq1	12	BITLUL	monomer
Sq2	5	761716[b]	chain
Ox1	3	415700	tetramer
Ox2	23	UYOXAL	monomer
Ox3	3	415698	dimer
Org1	31, 32	AMKCYB	
Org2	33	773267[b]	

[a] Unless otherwise noted, numeric codes are associated with the Inorganic Crystal Structure Database (ICSD) and literal codes with the Cambridge Structure Database (CSD). [b] CCDC deposition numbers used for structures that have not yet been assigned CSD reference codes.

hydroxyl group that bridges U1 and U2 (Figure 5b). The squarate anion consists of C1 and C2, with the remainder of the carbon ring generated by a mirror plane. The oxalate anion likewise sits on a mirror plane, with C3 and its symmetry equivalent forming the carbon component. The sheet that results from this coordination is shown in Figure 5a. It differs from that of **3** in the orientation of the uranyl cations. In both Figures 4a and 5a, two pairs of uranyl dimers have been outlined in bold. The uranyl cations of **3** alternately lean toward and away from each other, whereas those in **4** consistently lean toward each other. One water molecule (OW1) and one ammonium cation (N1) solvate the asymmetric unit. Important bond angles and distances are summarized in Table 3.

Powder X-Ray Diffraction. PXRD was used to identify the phases present in each synthesis and thus develop a more complete picture of the products under any given set of reaction conditions. The local structure of each identified species in the synthetic system is shown as a polyhedral representation in Figure 6, and references for previously reported structures may be found in Table 4. Reaction products in 1:1 and 1:2 metal to ligand ratio reactions are shown at appropriate temperature and pH ranges in Figures 7 and 8, respectively. Figure 9 shows products that form at 150 °C as a function of the pH and time. These data are additionally presented as powder

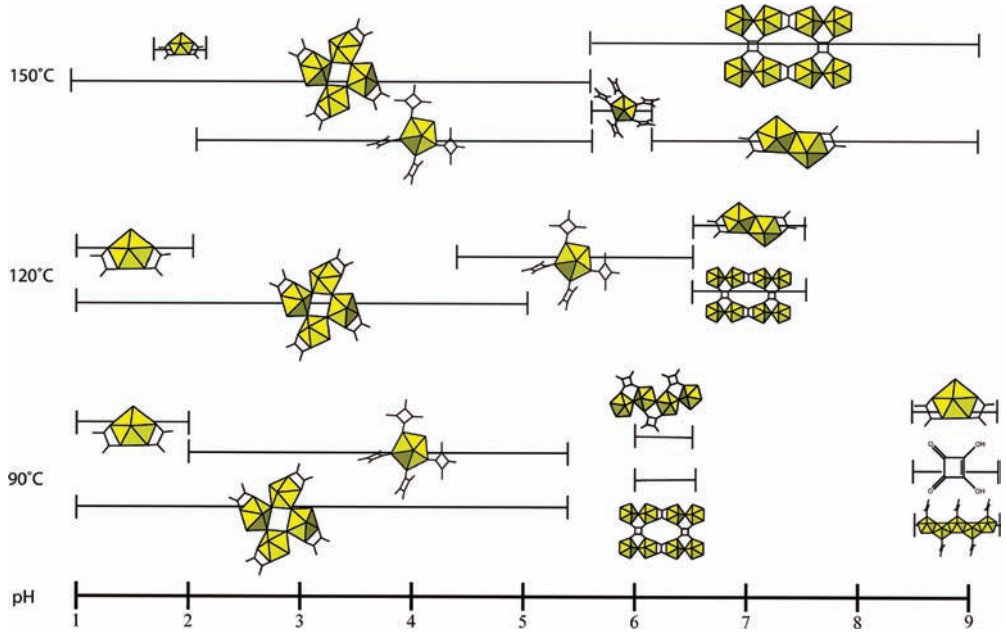

Figure 7. Polyhedral representation of the local structure of products from 1:1 metal to ligand ratio reactions over 3 days. Species are presented as a function of the temperature and initial pH. Refer to Figure 6 for a key to the local structures.

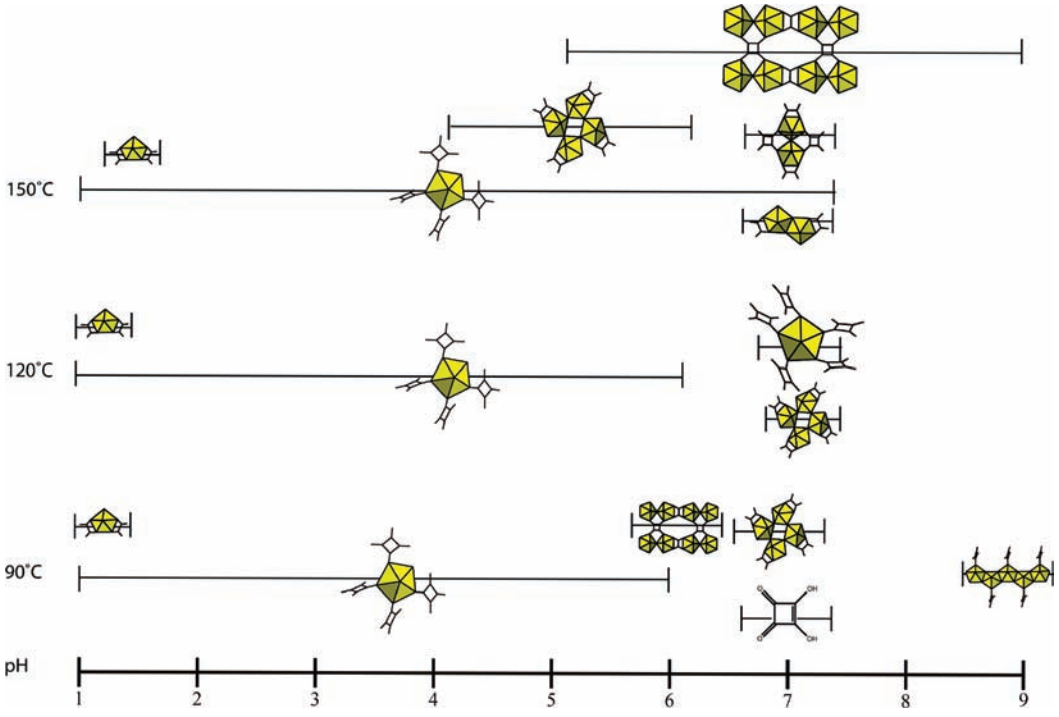

Figure 8. Polyhedral representation of the local structure of products from 1:2 metal to ligand ratio reactions over 3 days. Species are presented as a function of the temperature and initial pH. Refer to Figure 6 for a key to the local structures.

X-ray diffraction patterns in the Supporting Information (SI 2−9).

Discussion

Hydrolysis of the uranyl cation results in the formation of oligomers in solution. We have previously demonstrated that this hydrolysis translates into the solid state under ambient conditions in the form of oligomeric building units in uranyl squarates synthesized at relatively higher pH, while lower pH levels result in the formation of monomeric uranyl squarates.[5] Under hydrothermal conditions, however, hydrolysis has not been studied as thoroughly. Although we expect the hydrolysis equilibrium (eq 1) to continue to hold

(31) Peters, K.; Peters, E. M.; Schnering, H. G. v. *Acta Crystallogr., Sect. A* **1978**, *34*, S101.

(32) Georgopoulos, S. L.; Diniz, R.; Rodrigues, B. L.; Yoshida, M. I.; de Oliveira, L. F. C. *J. Mol. Struct.* **2005**, *753*, 147–153.

(33) Rowland, C. E.; Cahill, C. L. Private communication to the Cambridge Structural Database, deposition number CCDC 773276, **2010**.

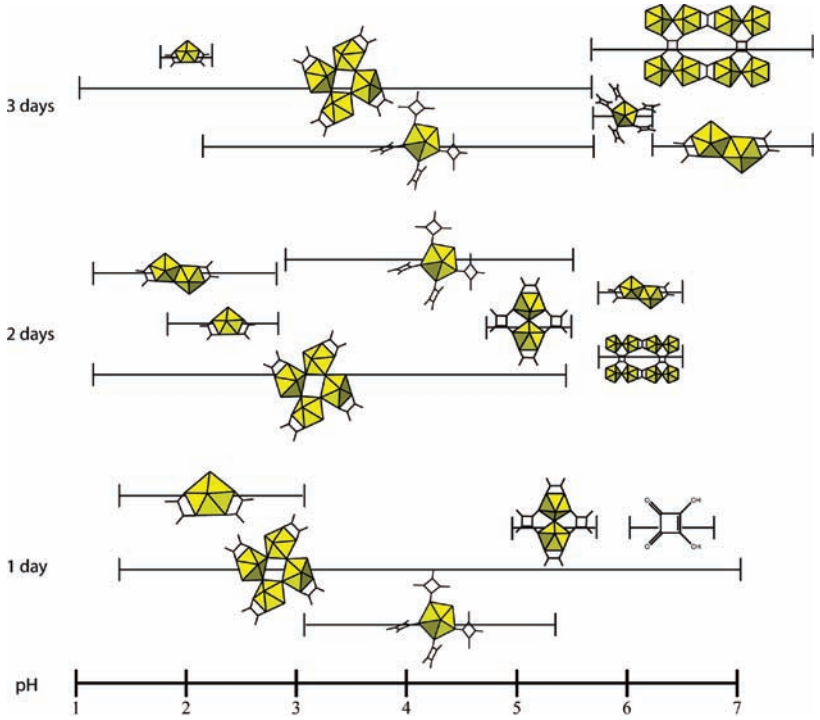

Figure 9. Polyhedral representation of the local structure of products from 1:1 metal to ligand ratio reactions at 150 °C. Species are presented as a function of the time and initial pH. Refer to Figure 6 for a key to the local structures.

true and thus anticipate oligomerization with increasing pH, previous studies of solutions indicate that monomeric hydroxide species are more prevalent than under ambient conditions.[6−8] The influence of temperature and pressure on uranyl hydrolysis is in fact quite complex. More species are observed in hydrothermal systems than under ambient conditions, and while monomeric species do displace some oligomeric species, they by no means dominate the solution. Under ambient conditions, monomers are most prevalent until approximately pH 5, and trimers dominate at higher pH.[6] At 100 °C, new monomeric species appear that displace some of the trimers both below pH 5 and above pH 6, but the oligomeric species continues to be the most prevalent in between.[8]

The manifestation of hydrolysis in solid state reaction products is visible in the crystal chemistry, in particular in the form of the uranyl building unit in the structure. In the squarate system under ambient conditions, oligomeric species first appear in the form of a trimer at pH 5.5, with a uranyl monomer persisting through pH 7.[5] Although we observe much greater structural diversity under hydrothermal conditions, a comparable trend holds true: oligomers first appear around pH 6, and monomers disappear by pH 7 (Figures 6 and 7). Looking specifically at the reaction series in which we use a 1:2 metal to ligand ratio (Figure 7), we note that Sq1 and Ox2 (monomers) dominate the species formed at low pH. As temperature increases, Sq1 persists to progressively higher pH, first disappearing at pH 4.5 at 90 °C but lasting through pH 7 by 150 °C. The re-emergence of a monomer (**1**) from pH 7−8 at 120 °C is consistent with the presence of a monomer in solution at higher pH with increasing temperature.[8] The oligomeric species, including **3**, **4**, Ox1, and Sq2, are generally observed at higher pH (above 6 for 90 °C, above 4 for 150 °C). It is also interesting—and perhaps not surprising—to note that at the highest temperature we explored, we observe increased decomposition of squaric acid to form oxalate products (Ox1, Ox2, **3**, and **4**) as compared to the lower temperature range.

In a 1:1 metal to ligand ratio (Figure 6), we also observe monomeric species that persist to pH 5, although here we do not see the increased range with increasing temperature that is evident in the 1:2 molar ratio. At pH > 6, the monomeric species have disappeared and oligomers (**2**, **3**, **4**, Sq2) appear. In contrast to this trend of oligomerization with increasing pH, however, a tetrameric oxalate species (Ox1) occurs from pH 1−5 over the full range of the temperatures that we explored. Although this species may be considered something of an anomaly in terms of uranyl hydrolysis, for reasons discussed below, we suggest that it may be a manifestation of a dynamic solution chemistry.

The appearance of both the squarate−oxalates, which we report here (**3** and **4**), and the previously reported oxalates (Ox1 and Ox2), though not intuitive, is unsurprising given previous reports of oxalate formation under hydrothermal conditions, where it has been observed from a variety of ligands,[13,17,34] including squaric acid.[18−20] Although hydrolysis of squaric acid to yield oxalic acid is reasonably straightforward, the introduction of this second species in the reaction is a significant complicating factor. First, hydrolysis of squaric acid liberates two equivalents of oxalic acid, thereby changing the overall metal to ligand ratio in the reaction vessel over time. Additionally, the affinities of squaric and oxalic acids for the uranyl cation are not necessarily identical. Thus, we must consider not only the generation of the second ligand but also the coordination preferences of both species, a difference in which could result in one ligand being "consumed" more readily than the other. Under ambient

(34) Ziegelgruber, K. L.; Knope, K. E.; Frisch, M.; Cahill, C. L. *J. Solid State Chem.* **2008**, *181*, 373–381.

conditions, we reported a certain metal to ligand ratio at the outset of a reaction and assumed that both UO_2^{2+} and squaric acid were consumed in tandem or that one disappeared at some fraction of the rate of the other (depending on the initial metal to ligand ratio and on the ratio in the product). With the generation of oxalate anions in situ, however, this is no longer the case. Hydrolysis and coordination behavior instead introduce a dynamic metal to ligand ratio that make it quite difficult to comment on metal hydrolysis to the exclusion of other factors contributing to product formation. As stated previously, we observe a *general* trend of monomeric species at lower pH, followed by the evolution of oligomeric species at higher pH, but the tetramer in Ox1 contradicts that trend over large pH and temperature ranges. Given the variety of factors contributing to the assembly of these materials, we believe that this anomaly may be driven by chemical forces other than hydrolysis. It is also interesting to note that we observe crystallization of unreacted squaric acid at low temperature and high pH in both 1:1 and 2:1 metal to ligand ratio systems. This appearance of crystalline squaric acid occurs in conjunction with uranyl oxalates and may perhaps be explained by an excess of ligand that results from the liberation of two equivalents of oxalic acid from every equivalent of squaric acid.

In addition to complicating the chemistry, the presence of oxalate in the products introduces a binding mode not observed previously in uranyl squarates. Although squarate anions have been known to chelate (coordinate in bidentate fashion), this coordination behavior has not been observed in uranyl chemistry. In contrast, oxalate anions chelate commonly, and this coordination mode is seen in both the squarate−oxalates (**3** and **4**) and oxalates (Ox1 and Ox2) that we observe. In order to determine whether chelation of a squarate anion to a uranyl pentagonal bipyramid was likely, we performed a search of the Cambridge Structural Database for squarate- and oxalate-containing compounds.[35,36] Only uranyl oxalates were included in the search, but the limited number of uranyl squarates required a broader search, so all d- and f-block metals coordinated in monodentate or bidentate squarate anions were included. Distance and angle parameters for the squarate and oxalate anions were defined as shown in Figure 10.[37]

The mean distance, *d*, for a monodentate squarate anion was 3.23 Å, for a bidentate squarate anion was 3.02 Å, and for an oxalate anion was 2.62 Å, values which correspond closely to the those that we observe in **1**−**4** (Table 3). We additionally established the distance between equatorial oxygen atoms on a uranyl pentagonal bipyramid (mean = 2.70 Å).[38] Only one of the search results shows a pentagonal bipyramid with a distance between adjacent oxygen atoms of greater than 3.1 Å. Thus while oxalate, with an interoxygen distance of 2.6 Å, fits easily into the typical interoxygen range for a uranyl pentagonal bipyramid and renders chelation a

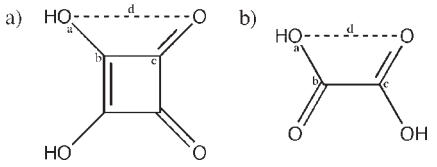

Figure 10. Distance and angle parameters defined as distance *d* and ∠*abc*, respectively, used in a search of the CSD performed for squarate and oxalate anions.

favorable coordination behavior, squarate, with a 3 Å distance, is too large to chelate readily to the uranyl cation. Chelation to a square bipyramid, which would possess slightly longer interoxygen distances, would be feasible, but this coordination geometry is less common for the uranyl cation and has not been observed anywhere in this synthetic system. Thus, the introduction of oxalate to this system permits a binding mode (i.e., chelation) that is not accessible in an exclusively squarate system.

The importance of a different binding mode can be considered in terms of product assembly, which we have stated is influenced by metal ion hydrolysis and organic coordination and geometry. The inorganic and organic species can be thought of as puzzle pieces that are only permitted to coordinate within geometric feasibility. As we have shown above, for example, a squarate anion is unlikely to chelate to a uranyl pentagonal bipyramid. Although the organic "piece" has only one shape, the inorganic component changes as a function of hydrolysis and oligomerization, which are responsible for the variety of building units that exist in solution under any given set of conditions. It is therefore reasonable to suppose that a ligand will coordinate to certain secondary building units more easily than to others simply by virtue of geometry. Once the building units have been pulled from solution upon crystallization, reestablishment of equilibrium would require that these be replenished.

Uranyl squarates have thus far consisted of monomers (**1** and Sq1), trimers,[5] and chains (**2** and Sq2). We know from previous studies, however, that other species exist in solution, including dimers, yet we do not observe dimeric uranyl squarates. Both squarate−oxalate structures (**3** and **4**), on the other hand, are composed of uranyl dimers. Perhaps the selection of dimers relies on the presence of oxalate. For example, a point-sharing dimer of pentagonal bipyramids is a linear species, which can easily be assembled into chains through the bisbidentate coordination that the oxalate anions exhibit, as in Figures 4 and 5. The addition of this third "puzzle piece" (i.e., oxalate anions) may facilitate the selection of dimers from solution.

Last, we also investigated the formation of uranyl oxalates by exploring a small set of reaction conditions as a function of time. Because in situ reactions likely do not occur instantaneously, we expected to see increasing levels of oxalate in our products over time. We instead observe a fairly steady level of oxalate products, as shown in Figure 8. The pH range over which the squarate anion remains intact in the formation of Sq1 and mixed squarate−oxalates also remains consistent as a function of the time (pH ∼3−7). Moreover, inspection of powder X-ray diffraction patterns shows little change in the level of squarates relative to oxalates (Supporting Information, SI 7−9). We can therefore say that oxalate formation occurs early in the reaction sequence, as hydrolysis of the squarate ion appears to have leveled off by the end of the first day.

(35) Allen, F. H. *Acta Crystallogr., Sect. B* **2002**, *58*, 380–389.
(36) *Cambridge Structural Database*, 1.12; CCDC: Cambridge, U.K., 2010.
(37) Squarate search was performed by specifying monodentate (1) or bidentate (2) coordination to any d- or f-block metal. Oxalate search was performed by specifying bidentate coordination to uranium (3). (1) 232 hits. Mean abc = 134.5°. Mean d = 3.23 Å. (2) 8 hits. Mean abc = 126.8°. Mean d = 3.02 Å. (3) 78 hits. Mean abc = 115.6°. Mean d = 2.62 Å.
(38) Search results for uranyl pentagonal bipyramids were manually screened for uranyl peroxides, which were excluded. From 216 hits, the mean distance interoxygen was 2.70 Å, minimum distance was 2.13 Å, maximum distance was 3.37 Å.

Conclusion

We have investigated the role of pH and temperature on ex situ expression of uranyl hydrolysis through the synthesis and crystallographic characterization of two new uranyl squarates (**1** and **2**) and two uranyl squarate−oxalates (**3** and **4**). We report a general trend of oligomerization with increasing pH, although we do note an important inconsistency in this trend with the formation of a tetrameric oxalate species at low pH. We do not observe any strong trend with increasing temperature. In addition to metal hydrolysis, we note the role of hydrolysis of squaric acid to oxalic acid in the assembly of **3**, **4**, and several previously reported uranyl oxalates.

Acknowledgment. This material is based upon work supported as part of the Materials Science of Actinides, an Energy Frontier Research Center funded by the U.S. Department of Energy, Office of Science, Office of Basic Energy Sciences under Award Number DE-SC0001089. Additional support was from the Chemical Sciences, Geosciences and Biosciences Division, Office of Basic Energy Sciences, Office of Science, Heavy Elements Program, U.S. Department of Energy, under Grant DE-FG02-05ER15736 at GWU. X-ray diffraction equipment was purchased with support from the National Science Foundation (DMR-0419754).

Supporting Information Available: Bond valence summation values for compounds **1**−**4** and powder X-ray diffraction patterns for reaction products as a function of pH are available free of charge via the Internet at http://pubs.acs.org. CIFs may also be obtained free of charge from The Cambridge Crystallographic Data Centre via www.ccdc.cam.ac.uk/data_request/cif by referencing CCDC 776027−776030.